12-29-2009

A High-Yield Synthesis of Chalcopyrite $CuInS_2$ Nanoparticles with Exceptional Size Control

Aaron Thurber
Boise State University

Alex Punnoose
Boise State University

Hindawi Publishing Corporation
Journal of Nanomaterials
Volume 2009, Article ID 748567, 7 pages
doi:10.1155/2009/748567

Research Article

A High-Yield Synthesis of Chalcopyrite $CuInS_2$ Nanoparticles with Exceptional Size Control

Chivin Sun,[1] Joseph S. Gardner,[2] Endrit Shurdha,[1] Kelsey R. Margulieux,[1] Richard D. Westover,[1] Lisa Lau,[1] Gary Long,[1] Cyril Bajracharya,[1] Chongmin Wang,[3] Aaron Thurber,[4] Alex Punnoose,[4] Rene G. Rodriguez,[1] and Joshua J. Pak[1]

[1] *Department of Chemistry, Idaho State University, Pocatello, ID 83209, USA*
[2] *Department of Physical Science, College of Southern Idaho, Twin Falls, ID 83303, USA*
[3] *W. R. Willey Environmental Molecular Sciences Laboratory, Pacific Northwest National Laboratory, Richland, WA 99352, USA*
[4] *Department of Physics, Boise State University, Boise, ID 83725, USA*

Correspondence should be addressed to Joshua J. Pak, pakjosh@isu.edu

Received 21 August 2009; Accepted 29 December 2009

Recommended by Theodore Tsotsis

We report high-yield and efficient size-controlled syntheses of Chalcopyrite $CuInS_2$ nanoparticles by decomposing molecular single source precursors (SSPs) via microwave irradiation in the presence of 1,2-ethanedithiol at reaction temperatures as low as 100°C and times as short as 30 minutes. The nanoparticles sizes were 1.8 nm to 10.8 nm as reaction temperatures were varied from 100°C to 200°C with the bandgaps from 2.71 eV to 1.28 eV with good size control and high yields (64%–95%). The resulting nanoparticles were analyzed by XRD, UV-Vis, ICP-OES, XPS, SEM, EDS, and HRTEM. Titration studies by ^{1}H NMR using SSP **1** with 1,2-ethanedithiol and benzyl mercaptan were conducted to elucidate the formation of Chalcopyrite $CuInS_2$ nanoparticles.

1. Introduction

Various I-III-VI_2 semiconductor materials have been identified as promising photovoltaic materials [1, 2]. Recently, quantum dot (QD) based solar cells have attracted much attention due to their potential to replace thin film devices [3–5]. One of the major advantages of employing QDs is by simply changing the particle size they can be tuned to absorb specific wavelengths ranging from visible to infrared wavelengths [6]. Furthermore, with careful design of photovoltaic (PV) devices incorporating various sizes of nanoparticles in multiple layers, one may achieve increased solar energy absorption in one device [7, 8]. In order to facilitate QD based multilayer devices, synthetic strategies that can deliver QDs in *high yields* with precise size control are essential. One of the strategies to prepare QDs is to prepare nanoparticles from molecular single source precursors (SSPs), which contain all necessary elements in a single molecule. In recent years, there have been several reports on the formation of $CuInS_2$ nanoparticles through the decomposition of SSPs using thermolysis [9–14], photolysis [15], and microwave irradiation [16]. However, many of these procedures require a combination of long reaction times (10 to 24 hours) and high reaction temperatures (often exceeding 200°C) with very little information regarding overall yields.

Microwave-assisted growth of nanoparticles is generally favorable over traditional thermolysis as microwave irradiation overcomes local intermediaries and increases the microscopic temperature of the reaction [17] thus exhibiting greater homogeneity in the overall reaction temperature. This allows for nanoparticles with diameters of a few nanometers to be prepared [18], dramatic decreases in reaction times, and improved product purities, all forms of precursors can be used, and reactions exhibit high reproducibility and yields [19].

For $CuInS_2$ QDs, the Wannier-Mott bulk exciton radius is approximately 8 nm with a bandgap of 1.45 eV and QDs with radii smaller than 8 nm exhibit bandgaps greater than 1.45 eV [20]. Our group has recently reported the synthesis of $CuInS_2$ nanoparticles using SSPs via microwave

irradiation with 1-hexanethiol as a surface pacifying ligand to afford nanoparticle sizes ranging from 3 to 5 nm [16]. Herein, we report efficient size controlled syntheses of Chalcopyrite $CuInS_2$ nanoparticles by decomposition of SSPs in the presence of 1,2-ethanedithiol with extraordinarily high yields. The titration studies by ^{1}H NMR using SSP **1** with 1,2-ethanedithiol and benzyl mercaptan are conducted to elucidate the formation of Chalcopyrite $CuInS_2$ nanoparticles.

2. Experimental

The single source precursor (SSP **1**), $(Ph_3P)_2Cu(\mu\text{-}SEt)_2In(SEt)_2$, was synthesized according to literature [21]. For preparing nanoparticles, in general, in a dry Milestone microwave vessel, $(Ph_3P)_2Cu(\mu\text{-}SEt)_2In(SEt)_2$ (1.0 g, 1.1 mmol) was dissolved in 8.0 mL of dioctyl phthalate (DOP) or benzyl acetate followed by addition of 1,2-ethanedithiol (0.6 mL, 7.7 mmol). The solution was capped and stirred for 5 minutes at room temperature. The reaction mixture was then irradiated with microwave irradiation achieving reaction temperatures from 100°C to 200°C as desired for less than 2 hours. Upon completion, the reaction was cooled to room temperature to yield precipitation of $CuInS_2$ nanoparticles. The resulting nanoparticles were isolated from the DOP or benzyl acetate solution by centrifugation, collected, and washed three times with CH_3OH. The product was then dried in *vacuo* to provide yellow to black powder. This method has been successfully adapted to prepare up to 5 g of nanoparticles in a single vessel.

Milestone Microwave (Labstation Terminal 320) was used with a 15-minute ramp and a 15–120-minute hold at desired reaction temperatures. The resulting nanoparticles were characterized using a Leo Model 1430-VP scanning electron microscope (SEM) with an Oxford Model 7353 electron dispersive spectroscopy (EDS) attachment employing Inca Software, and a JEOL 2010 high-resolution transmission electron microscope (HRTEM) with a spatial resolution of 0.194 nm. Powder X-ray diffraction (XRD) patterns were acquired with a Bruker D8 Discover diffractometer using CuKa radiation and a scintillation detector. Scans were collected for 4 hours employing a 0.06° step width at a rate of 10 s/step resulting in a 2θ scan range from 10 to 60°.

Absorption spectra of nanoparticles were obtained from UV-Vis data recorded on a PerkinElmer Lambda 35 spectrophotometer using an integrating sphere module at room temperature. Inductively Coupled Plasma-Optical Emission Spectroscopy (ICP-OES) analysis was accomplished by weighing 10 mg of each nanoparticle sample then digesting in concentrated HNO_3 to make a 10 ppm solution. All samples were run within 24 hours of preparing the solution to ensure that the results were consistent. All ICP data were recorded on a Varian 715-ES (ICP-OES with V-groove Nebulizer).

X-ray Photoelectron Spectroscopy (XPS) data were recorded on a Physical Electronics Versaprobe. Samples were irradiated with a monochromated Al Kα x-ray beam approximately 100 μm in diameter at about 25 watts. Powder samples were mounted using double-sided carbon conductive tape attached to Si wafer fragments. To prevent electrical charging, the system used a dual beam neutralization comprised of a flood of 10 eV electrons and a focused beam of 10 eV Ar^+ ions. The spectrometer pass energy was set at 117.5 eV for the survey scans and 23.5 eV for the high-resolution spectra, and the binding energy scale was calibrated using the Cu $2p_{3/2}$ and Au $4f_{7/2}$ peaks from freshly sputter cleaned 99.9% pure Cu and Au foils. The spectrometer acceptance window was oriented for a take-off angle of 45° off the sample normal. Sputter cycles of 2 kV Ar^+ ions with a current of 1 μA rastered over a 2 mm × 2 mm area were performed in 60-second intervals for a total of 4 minutes of sputtering. The sputtering rate at these settings was calibrated to ~4.7 nm/min for SiO_2. The high-resolution data have been shifted referencing the 284.5 eV C 1 s peak.

A ^{1}H NMR titration study of SSP **1** with $HSCH_2CH_2SH$ was conducted using solutions of $(Ph_3P)_2Cu(\mu\text{-}SEt)_2In(SEt)_2$ (465 mg, 0.491 mmol) with $C_6H_3(OCH_3)_3$ (12.3 mg, 0.0731 mmol) as an internal standard in 6.00 mL C_6D_6, and $HSCH_2CH_2SH$ (25.0 μL, 0.298 mmol) in 339 μL C_6D_6 for final molarities of 0.08182, 0.01219, and 0.8189 M, respectively. All volumes were measured using small volume precision syringes. To each NMR tube 0.200 mL $(Ph_3P)_2Cu(\mu\text{-}SEt)_2In(SEt)_2$ solution was delivered, followed by appropriate volume of thiol solution and the necessary volume of C_6D_6 to raise final solution volume to 0.550 mL. All ^{1}H NMR spectra were recorded on a JEOL ECX-300A spectrometer. Chemical shifts were referenced relative to residual benzene-d_6 peak (^{1}H, δ 7.160). The ^{1}H NMR titration study of SSP **1** with $HSCH_2Ph$ was prepared analogously to $HSCH_2CH_2SH$.

3. Results and Discussion

A typical nanoparticle preparation used an SSP, such as $(Ph_3P)_2Cu(\mu\text{-}SEt)_2In(SEt)_2$ (**1**), which was decomposed via microwave irradiation in the presence of 1,2-ethanedithiol as a surface stabilizing ligand. Surprisingly, when employing 1,2-ethanedithiol instead of 1-hexanethiol [16], we discovered that $CuInS_2$ nanoparticles can be produced with good size control in high yields (64%–95% based on ICP-OES data) at very short reaction time (Table 1). Figure 1 shows the resulting nanoparticles that settled in the bottom of sample vessels. Progressively darker colors are the results of higher reaction temperatures representing respective sizes of $CuInS_2$ nanoparticles from small to large. According to EDS data (Table 1), all particles formed in our studies consist of Cu, In, and S. Additional information gathered from XPS (Figure 2 and Table 2) and ICP (Table 1) indicates that the nanoparticles have approximate atomic ratio of 1 : 1 : 2 confirming the chemical composition of $CuInS_2$ independent of reaction temperatures and nanoparticle sizes.

SEM images (Figure 3) of $CuInS_2$ nanoparticles show micron scale coral like morphology. One of the interesting aspects of these samples is that when nanoparticles are formed in the presence of 1,2-ethanedithiol, the particles undergo extensive three dimensional networking. This

Table 1: Percent yields of nanoparticles by ICP-OES prepared by increasing reaction temperature.

Entry*	Reaction Temp.	Mass of isolated NP**	NP and pacifying agent***	Result from ICP		Cu : In ratio		ICP corrected yield of CIS
				Cu	In			
	°C	mg	mg	mg	mg	ICP	EDS	%
1	100	340	10.60	1.44	2.59	1.01	1.08	63.8 ± 4.6
2	120	292	10.21	1.58	2.82	1.01	1.03	65.0 ± 2.0
3	140	273	10.07	2.02	3.41	1.07	1.13	77.0 ± 2.4
4	160	267	10.21	2.36	3.75	1.14	1.18	85.4 ± 3.9
5	180	257	10.30	2.44	3.91	1.13	1.21	83.6 ± 4.4
6	200	243	10.90	3.01	5.06	1.08	1.05	94.8 ± 3.6

*Reaction condition: using 1.00 g SSP **1**, 8.00 mL solvent, and 0.60 mL $HSCH_2CH_2SH$ at 105 minutes.
Isolated mass of nanoparticle from 1 g of SSP **1 plus the pacifying agent (1,2-ethanedithiol).
***Quantities of NPs used for ICP-OES analysis.

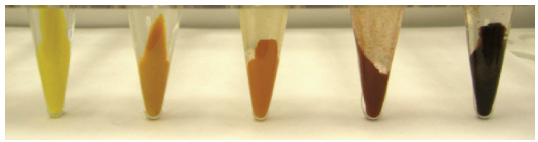

Figure 1: $CuInS_2$ nanoparticles prepared from SSPs in presence of 1,2-ethanedithiol in DOP at 130, 140, 150, 160, and 170°C, respectively, from left to right.

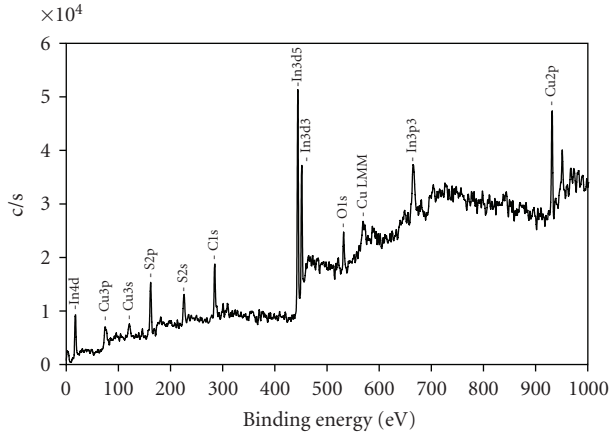

Figure 2: XPS data of a $CuInS_2$ nanoparticle produced at 160°C.

Table 2: Atomic percents and ratios by XPS of a $CuInS_2$ nanoparticle produced at 160°C.

Sputtering time (min)	Cu (%)	In (%)	S (%)	Cu : In ratio	S : (Cu+In) ratio
0	24.2	23.9	51.9	1.01	1.08
1	25.8	25.4	48.8	1.02	0.95
2	26.7	25.6	47.7	1.04	0.91
3	25.6	26.9	47.5	0.95	0.90
4	27.7	29.0	43.3	0.96	0.76

behavior is attributed to the thiol/thiolate interactions (Figures 10 and 11).

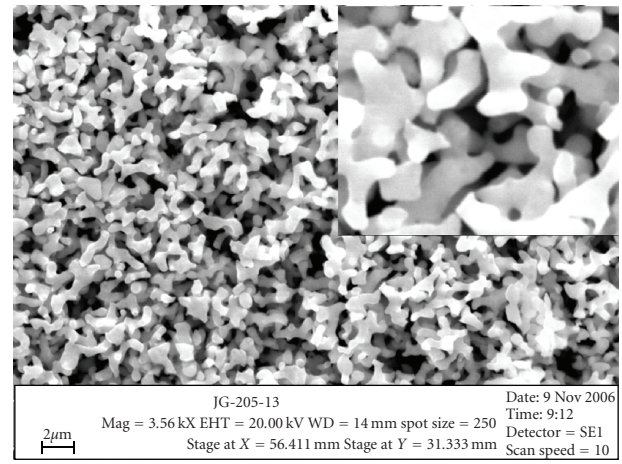

Figure 3: SEM image of $CuInS_2$ nanoparticles at 160°C in a coral like morphology.

Upon further magnification, we found the coral like structures were the result of extensive cross-linked particles which make larger clusters and bundles (Figures 4(a) and 4(b)). The size distribution of our nanoparticles was difficult to determine due to their complex cross-linked structures (Figure 4(c)). By our best estimation, the nanoparticles appear to have about 4 nm diameters with narrow size distribution as shown in Figure 4(c).

From the XRD data, we determined volume-weighted crystal diameters (Scherrer equation with a shape factor of 0.9) [22] of our samples range from 1.8 nm to 10.8 nm as the reaction temperatures increased from 100°C to 200°C (Figure 5).

The nanoparticle sizes from 1.8 nm to 10.8 nm (yellow to black) were confirmed by evaluation of HRTEM images. The XRD patterns show the $CuInS_2$ nanoparticles are crystalline with the Chalcopyrite phase with major peaks at $2\theta = 28$, 46, and 55°. The peaks are consistent with tetragonal $CuInS_2$ reference pattern 85-1575 (JCPDS-03-065-2732). Furthermore, a careful evaluation of the gradual sharpening of the peaks in the XRD spectra is indicative of the increasing particle sizes with increasing reaction temperatures (Figure 5).

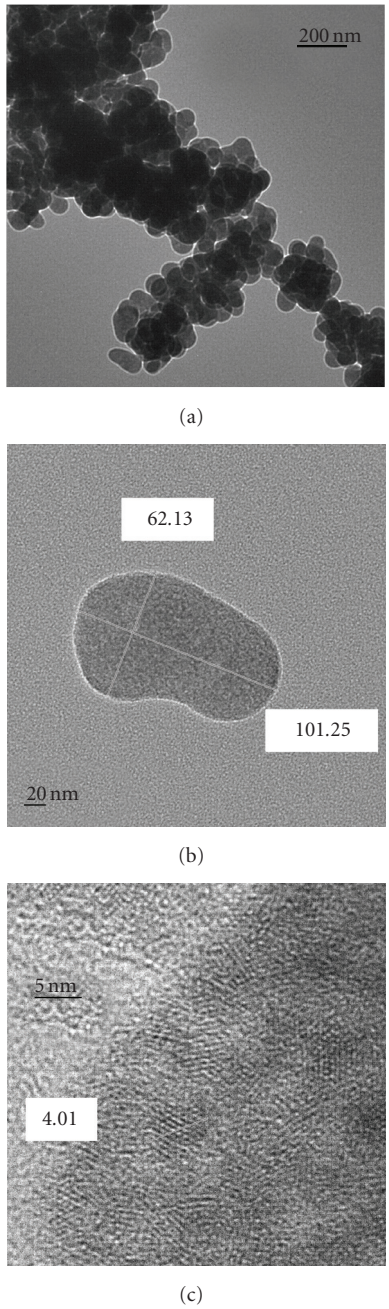

FIGURE 4: HRTEM images of $CuInS_2$ nanoparticles at 160°C: (a) bundle of clusters, (b) nanoparticle cluster, and (c) individual nanoparticles in the cluster.

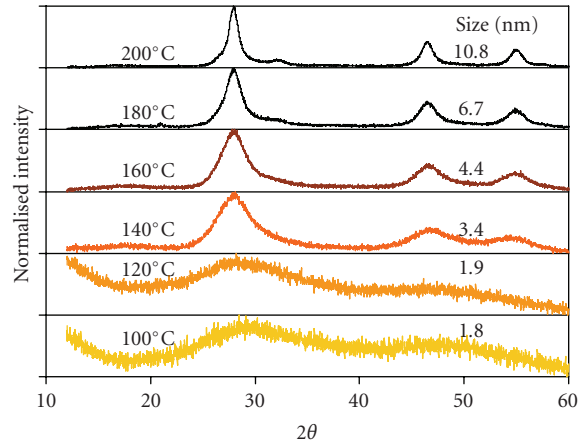

FIGURE 5: Normalized XRD data of $CuInS_2$ nanoparticles prepared from 100 to 200°C, respectively, with calculated diameters.

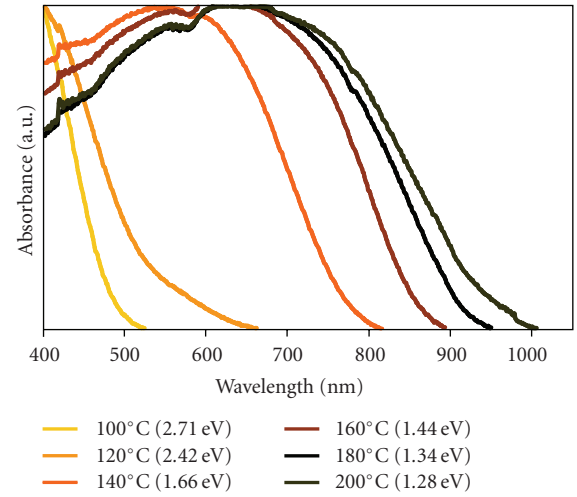

FIGURE 6: Normalized UV-Vis absorption spectra of typical $CuInS_2$ nanoparticles prepared from 100 to 200°C, respectively, with calculated bandgaps.

The absorption behaviors of the nanoparticles showed the expected blue-shift with decreasing sizes and reaction temperatures which represent small to large bandgaps (Figure 6).

We observed further that size control is highly dependent on the presence of 1,2-ethanedithiol (Figure 7). In the absence of 1,2-ethanedithiol, Chalcopyrite nanoparticles were not produced (Figure 7(a)) [10]. It was determined that at least one equivalence of 1,2-ethanedithiol was required to produce Chalcopyrite nanoparticles. When neat 1,2-ethanedithiol was used as the reaction solvent at 140°C, the largest Chalcopyrite nanoparticles were collected (Figure 7(e)). The UV-Vis spectra show that blue-shift upon decreasing the size of the nanoparticles as 1,2-ethanedithiol is decreased from neat to 0.00 mL at constant SSP **1** concentration, temperature, and reaction time (Figure 8). At a given isotherm, reaction times were increased from 15 to 120 minutes, and very little differences were observed in nanoparticle sizes or yields (Figure 9).

Despite the clear usefulness of 1,2-ethanedithiol in the production of $CuInS_2$ nanoparticles, the precise mechanism for the dramatic reduction in reaction temperatures and times, along with high yields, is not yet known. Our hypothesis involves 1,2-ethanedithiol acting as a bridging unit between two SSP units, if it can exchange with ethane thiolate moieties in the SSP. Potentially, this process could occur multiple times to produce highly cross-linked oligomeric structures which would undergo rapid decomposition to

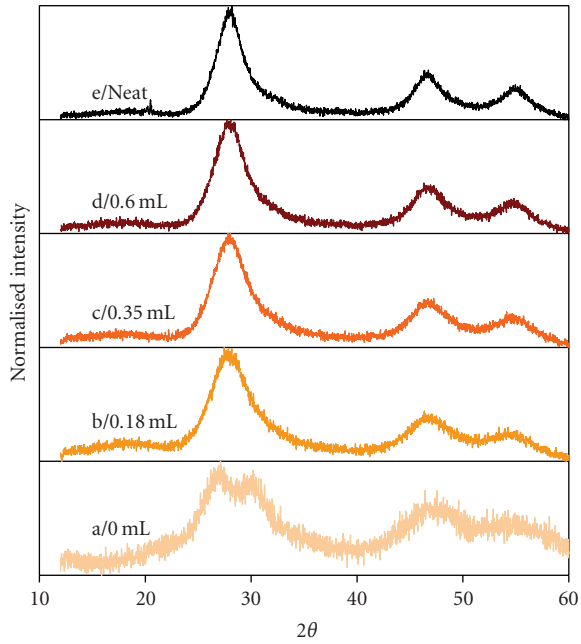

Figure 7: Normalized XRD data of $CuInS_2$ nanoparticles prepared from variation of 1,2-ethanedithiol concentrations.

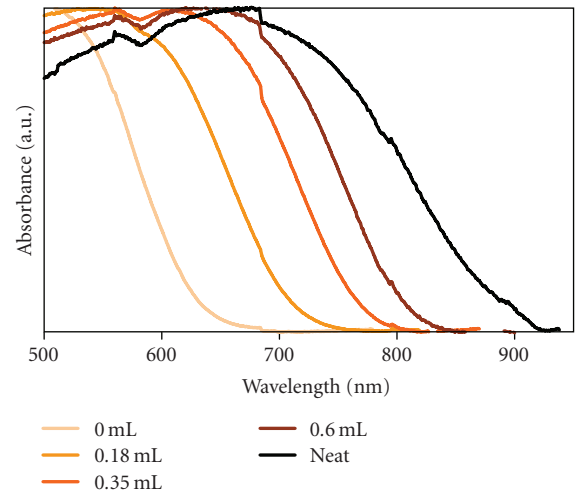

Figure 8: Normalized UV-Vis absorption spectra of $CuInS_2$ nanoparticles prepared from variation of 1,2-ethanedithiol concentrations.

produce the resulting $CuInS_2$ nanoparticles. This oligomeric unit would explain our low reaction temperatures, short reaction times, and high yields, as the nucleation and growth of the nanoparticles would happen over much shorter distances.

In order to elucidate this hypothesis, we conducted titration studies of SSP **1** with 1,2-ethanedithiol (Figure 10). For comparison, we selected benzyl mercaptan as a bulky monothiol (Figure 11). The ^{1}H NMR spectra of these titration studies clearly show that ethane thiolate moieties in SSP **1** exchange readily with added free thiols.

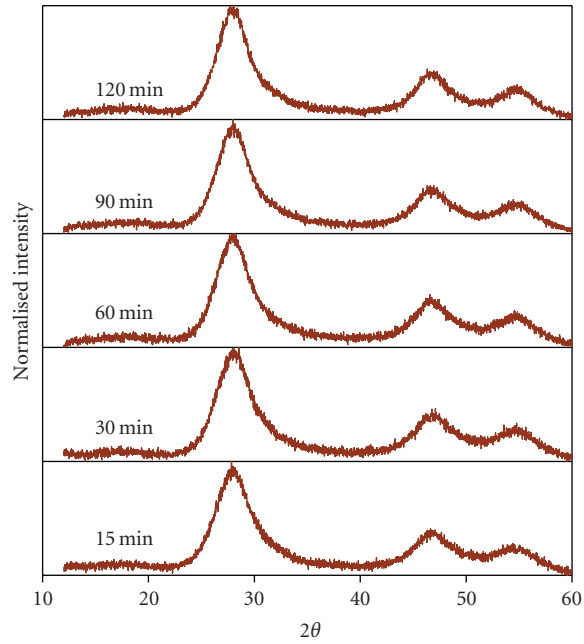

Figure 9: Normalized XRD data of $CuInS_2$ nanoparticles prepared from variation of reaction times at 140°C.

The proton resonances of SSP **1** appear at δ 1.39 ppm (12H, t, CH_3–), δ 2.98 ppm (8H, q, –CH_2–S), δ 7.05 ppm (18H, m, Ph), and δ 7.47 ppm (12H, t, br, Ph) in benzene. ^{1}H NMR of the aryl regions of SSP **1** was not shown (Figures 10 and 11). As increasing amounts of 1,2-ethanedithiol were added to SSP **1**, the new resonances of free $HSCH_2CH_3$ appearing at δ 0.9 ppm (3H, t, CH_3–), δ 1.1 ppm (1H, t, HS–), and δ 2.0 ppm (2H, q, –CH_2S–) were observed. In addition, the disappearance of resonances at δ 1.39 ppm and δ 2.98 ppm, which represent M-SCH_2CH_3, confirms the loss of bound ethane thiolate. Furthermore, the exchange between 1,2-ethanedithiol and ethane thiolate reaches saturation point at 2 : 1 ratio of 1,2-ethanedithiol to SSP **1**, as expected. This is clearly evident as we observe free 1,2-ethanedithiol resonances beyond the saturation point.

After the addition of more than 2 equivalents of 1,2-ethanedithiol, we observed formation of white precipitate, which we believe is the oligomeric species of SSP. When these white precipitates were irradiated with microwave, we were able to isolate analogous $CuInS_2$ nanoparticles. We are currently investigating formation of possible oligomeric species.

The observation of the titration of SSP **1** with 1,2-ethanedithiol is analogous to the titration of SSP **1** with benzyl mercaptan. As increasing amounts of benzyl mercaptan were added to SSP **1**, we observed new resonances of free $HSCH_2CH_3$ appearing at δ 0.9 ppm (3H, t, CH_3–), δ 1.1 ppm (1H, t, HS–), and δ 2.0 ppm (2H, q, –CH_2S–). In addition, we observed the increase of new resonance at δ 4.2 ppm of M-SCH_2Ph (benzyl mercaptan bound to the metal of SSP **1**). The disappearance of resonances of M-SCH_2CH_3 at δ 1.39 ppm and δ 2.98 ppm confirms the loss of ethane thiolate. At 4 equivalents, the lack of the M-SCH_2CH_3

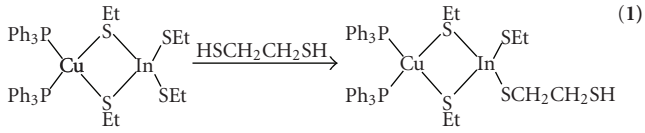

(a)

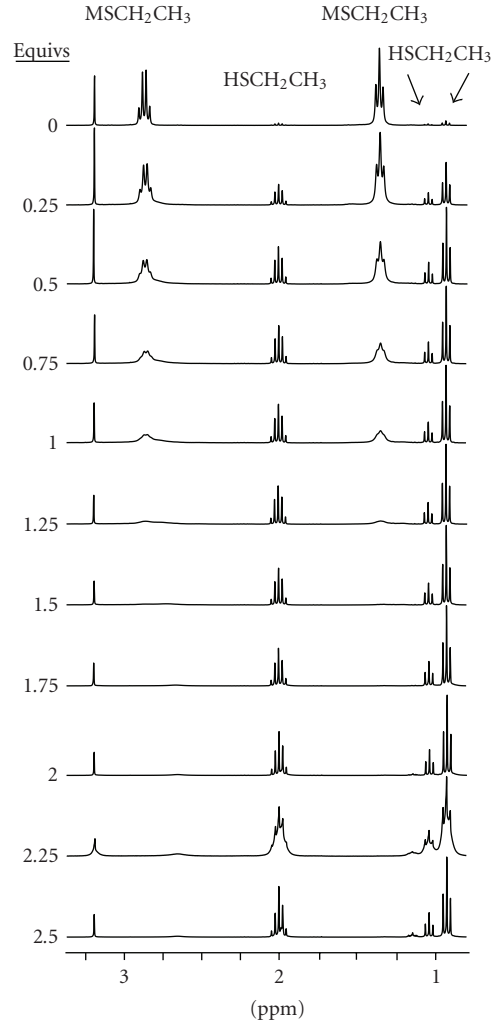

(b)

Figure 10: ^{1}H NMR spectra showing the titration of SSP **1** with 1,2-ethanedithiol. The δ 3.2 ppm is an internal standard.

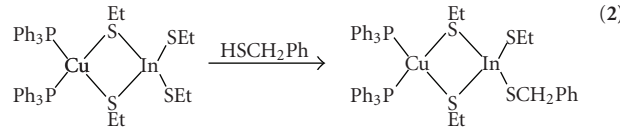

(a)

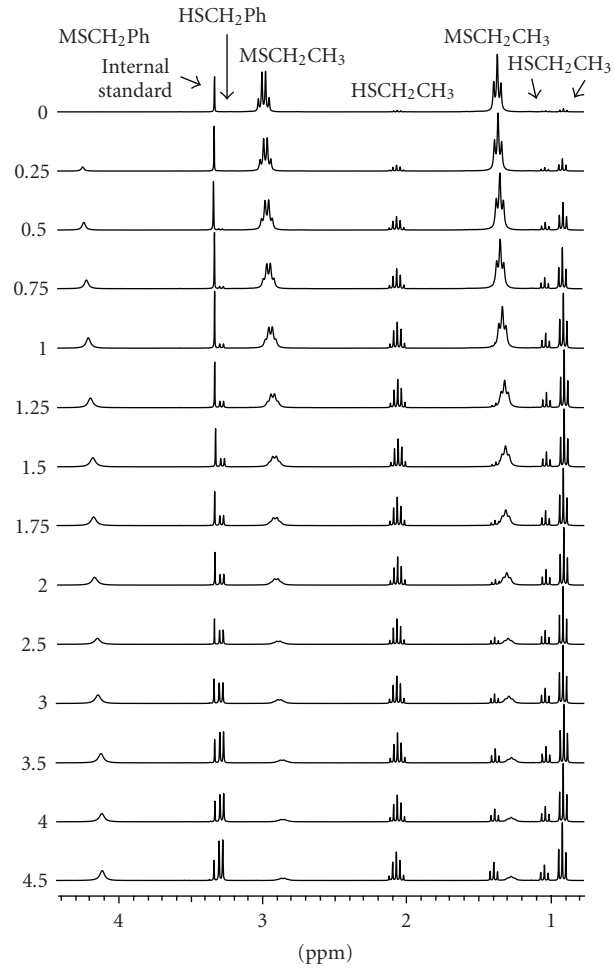

(b)

Figure 11: ^{1}H NMR spectra showing the titration of SSP **1** with benzyl mercaptan.

resonance indicates that most of the M-SCH_2CH_3 is replaced by benzyl mercaptan to form M-SCH_2Ph.

4. Conclusion

We have shown that by exploiting the microwave decomposition of single source precursors of $CuInS_2$ in the presence of 1,2-ethanedithiol, we can prepare $CuInS_2$ nanoparticles with diameters ranging from 1.8–10.8 nm with good size control and very high yields. Short reaction times of 2 hours or less are required for the preparation of these nanoparticles. The reaction temperature, 1,2-ethanedithiol concentration, and reaction time are all critical for fine control of nanoparticle size. The ^{1}H NMR has shown that the ethane thiolate moiety in the SSP **1** exchanges readily with addition of 1,2-ethanedithiol and benzyl mercaptan, supporting our hypothesis for 1,2-ethanedithiol acting as a bridging unit for highly cross-linked oligomeric structures.

Acknowledgments

The authors would like to thank DOE for financial support through the EPSCoR Grant no. DE-FG02-04ER46142 and instrument acquisition from NSF-MRI award 0722699. The HRTEM data was gathered using EMSL, a national scientific user facility sponsored by the Department of Energy's Office of Biological and Environmental Research and located at Pacific Northwest National Laboratory.

References

[1] J.-F. Guillemoles, L. Kronik, D. Cahen, U. Rau, A. Jasenek, and H.-W. Schock, "Stability issues of Cu(In,Ga)Se_2-based solar cells," *Journal of Physical Chemistry B*, vol. 104, no. 20, pp. 4849–4862, 2000.

[2] A. Rockett and R. W. Birkmire, "$CuInSe_2$ for photovoltaic applications," *Journal of Applied Physics*, vol. 70, no. 7, pp. R81–R97, 1991.

[3] G. Wei and S. R. Forrest, "Intermediate-band solar cells employing quantum dots embedded in an energy fence barrier," *Nano Letters*, vol. 7, no. 1, pp. 218–222, 2007.

[4] R. D. Schaller and V. I. Klimov, "High efficiency carrier multiplication in PbSe nanocrystals: implications for solar energy conversion," *Physical Review Letters*, vol. 92, no. 18, Article ID 186601, 4 pages, 2004.

[5] N. G. Anderson, "Ideal theory of quantum well solar cells," *Journal of Applied Physics*, vol. 78, no. 3, pp. 1850–1861, 1995.

[6] R. P. Raffaelle, S. L. Castro, A. F. Hepp, and S. G. Bailey, "Quantum dot solar cells," *Progress in Photovoltaics*, vol. 10, no. 6, pp. 433–439, 2002.

[7] A. Kongkanand, K. Tvrdy, K. Takechi, M. Kuno, and P. V. Kamat, "Quantum dot solar cells. Tuning photoresponse through size and shape control of CdSe-TiO_2 architecture," *Journal of the American Chemical Society*, vol. 130, no. 12, pp. 4007–4015, 2008.

[8] N. C. Swe, O. Tangmattajittakul, S. Suraprapapich, et al., "Improved quantum confinement of self-assembled high-density InAs quantum dot molecules in AlGaAsGaAs quantum well structures by molecular beam epitaxy," *Journal of Vacuum Science and Technology B*, vol. 26, no. 3, pp. 1100–1104, 2008.

[9] S. L. Castro, S. G. Bailey, R. P. Raffaelle, K. K. Banger, and A. F. Hepp, "Synthesis and characterization of colloidal $CuInS_2$ nanoparticles from a molecular single-source precursor," *Journal of Physical Chemistry B*, vol. 108, no. 33, pp. 12429–12435, 2004.

[10] S. L. Castro, S. G. Bailey, R. P. Raffaelle, K. K. Banger, and A. F. Hepp, "Nanocrystalline chalcopyrite materials ($CuInS_2$ and $CuInSe_2$) via low-temperature pyrolysis of molecular single-source precursors," *Chemistry of Materials*, vol. 15, no. 16, pp. 3142–3147, 2003.

[11] K. K. Banger, M. H.-C. Jin, J. D. Harris, P. E. Fanwick, and A. F. Hepp, "A new facile route for the preparation of single-source precursors for bulk, thin-film, and nanocrystallite I-III-VI semiconductors," *Inorganic Chemistry*, vol. 42, no. 24, pp. 7713–7715, 2003.

[12] S. Han, M. Kong, Y. Guo, and M. Wang, "Synthesis of copper indium sulfide nanoparticles by solvothermal method," *Materials Letters*, vol. 63, no. 13-14, pp. 1192–1194, 2009.

[13] H. Zhong, Y. Zhou, M. Ye, et al., "Controlled synthesis and optical properties of colloidal ternary chalcogenide $CuInS_2$ nanocrystals," *Chemistry of Materials*, vol. 20, no. 20, pp. 6434–6443, 2008.

[14] D. P. Dutta and G. Sharma, "A facile route to the synthesis of $CuInS_2$ nanoparticles," *Materials Letters*, vol. 60, no. 19, pp. 2395–2398, 2006.

[15] J. J. Nairn, P. J. Shapiro, B. Twamley, et al., "Preparation of ultrafine chalcopyrite nanoparticles via the photochemical decomposition of molecular single-source precursors," *Nano Letters*, vol. 6, no. 6, pp. 1218–1223, 2006.

[16] J. S. Gardner, E. Shurdha, C. Wang, L. D. Lau, R. G. Rodriguez, and J. J. Pak, "Rapid synthesis and size control of $CuInS_2$ semi-conductor nanoparticles using microwave irradiation," *Journal of Nanoparticle Research*, vol. 10, no. 4, pp. 633–641, 2008.

[17] J. A. Gerbec, D. Magana, A. Washington, and G. F. Strouse, "Microwave-enhanced reaction rates for nanoparticle synthesis," *Journal of the American Chemical Society*, vol. 127, no. 45, pp. 15791–15800, 2005.

[18] J. Zhu, O. Palchik, S. Chen, and A. Gedanken, "Microwave assisted preparation of CdSe, PbSe, and $Cu_{2-x}Se$ nanoparticles," *Journal of Physical Chemistry B*, vol. 104, no. 31, pp. 7344–7347, 2000.

[19] H. Grisaru, O. Palchik, A. Gedanken, V. Palchik, M. A. Slifkin, and A. M. Weiss, "Microwave-assisted polyol synthesis of $CuInTTe_2$ and $CuInSe_2$ nanoparticles," *Inorganic Chemistry*, vol. 42, no. 22, pp. 7148–7155, 2003.

[20] C. Czekelius, M. Hilgendorff, L. Spanhel, et al., "A simple colloidal route to nanocrystalline ZnO/$CuInS_2$ bilayers," *Advanced Materials*, vol. 11, no. 8, pp. 643–646, 1999.

[21] W. Hirpo, S. Dhingra, A. C. Sutorik, and M. G. Kanatzidis, "Synthesis of mixed copper-indium chalcogenolates. single-source precursors for the photovoltaic materials CuInQ2 (Q = S, Se)," *Journal of the American Chemical Society*, vol. 115, no. 4, pp. 1597–1599, 1993.

[22] H. Natter, M. Schmelzer, M.-S. Löffler, C. E. Krill, A. Fitch, and R. Hempelmann, "Grain-growth kinetics of nanocrystalline iron studied in situ by synchrotron real-time X-ray diffraction," *Journal of Physical Chemistry B*, vol. 104, no. 11, pp. 2467–2476, 2000.